Modeling, fabrication and investigation of mixing in low-cost passive PDMS micromixers

T Pravinraj, Rajendra Patrikar
Center for VLSI and Nanotechnology
Visvesvaraya National Institute of Technology
Nagpur, India
pravinraj1711@gmail.com

Abstract—In this work, a lattice Boltzmann method (LBM) modeling and investigation of mixing in a low-cost poydimethylsiloxane (PDMS) micromixer has been discussed. The PDMS micromixers are fabricated using simple printed circuit board (PCB) mold by eliminating the need of UV-lithography and plasma chamber. Thus a low-cost methodology to fabricate a micromixer has been presented. The fabricated device is modeled using mesoscopic LBM and investigation of mixing efficiency is done. Six different passive micromixers with different obstacle pattern are fabricated and characterized using in-house developed characterization system. The result shows that the pattern having more sharp edges along with the roughness provides maximum enhancement of the mixing efficiency. The obtained results can be utilized to design an efficient micromixer for lab-on-a-chip applications.

Keywords—lattice Boltzmann method(LBM); micromixer; PCB mold; low-cost; lab-on-a-chip;

I. INTRODUCTION

Miniaturization of the structures and devices provides tremendous advantages like high speed, portability, low power and compactness. As the devices are becoming small ever, the surface to volume ratio (S/V) in these devices increases sharply and hence it is now a crucial phenomenon in determining characteristics and performance of the devices. For example, the manipulation of fluids in micro and nano scale is emerged as the challenging task[1]. Controlling the smaller volume of fluid is preferable in many useful applications such as lab-on-chip (LOC)[2]. In the past decade, the droplet based microfluidics are getting popular over the conventional microfluidics[3], [4]. However, in practice, the conventional microfluidic devices offer simple solution without unwanted side effects on the study due to external electric voltage or current[5]. In a typical LOC device, the sizes of the microchannels are extremely small and the fluid flow rate is expected to be low[6]. Moreover the turbulence inside such microchannel is usually unnoticed and mostly the flow remains laminar due to the dimensionless Reynolds number is in the order of 10^{-3}. This raises the critical challenge for achieving the good mixing in many applications. So design and optimization of mixing devices for such applications has now emerged as an interesting research problem. Active micromixers achieve mixing through the external forces such as pressure driven, acoustic driven, temperature-induced or magneto-hydrodynamic[7]–[9]. The actuation of fluids through electro kinetic phenomenon[10], [11] is also popular in research. But it requires a high voltage supply and uses charged surface for electro-osmotic flow. This restricts the kind of material that can be used. Moreover, there exists a possibility that such high electric field can directly damage the medium of interest such as cell structure, antibodies and other body fluid components. In such cases, pneumatic actuation may be preferred with portability. But they need to be operated in low flow rate with precise control. Thus the active micromixers have practical limitations such as complex and expensive fabrication process. On the other hand, the passive micromixers rely on the mass transport phenomena provided by molecular diffusion and chaotic advection. They are simple, safe and easier to incorporate in the microscale. These devices are designed with a suitable channel geometry and topography that decreases the path width for diffusion and increases the surface contact area between the different fluids. By a suitable channel design, the chaotic advection can be realized by allowing the manipulation of the laminar flow inside the channels. Geometry and topography based passive mixers such as Y-mixer, T-Mixer, serpentine mixer are already exists and well studied in past [12]. However, the investigations on hybrid geometries including various structures are being explored to enhance the performance such as mixing time, length and mixing efficiency.

For fabrication of such devices, new materials such as polydimethylsiloxane (PDMS), polymethylmethacralate (PMMA) and other such polymers are preferred than the traditional MEMS materials such as Silicon, quartz etc. It also provides the various advantages like the better visibility, flexibility, bio-compatibility and low-cost. Usually, to fabricate such microfluidic devices, a popular soft-lithography technique based on UV-lithography is used. In this method, a photoresist (SU-8) mold is usually created using UV-lithography and for bonding the channel with the glass, plasma is used in a highly sophisticated clean room environment[13]. However, most clean room environment prevents the usage of

2380-6923/19/$31.00 ©2019 IEEE
DOI 10.1109/VLSID.2019.00051

non-CMOS compatible materials in their labs due to issues like contamination and maintenance. The establishment of UV-lithography setups and maintenance is not easily affordable for many LOC researchers and labs. Moreover, characterization of such devices is also a challenging task.

Most of the CAD tools require a mathematical model based on the physical phenomenon validated by the experimental result. This model is usually then used for computer simulations to validate design. Generally to model such a multiphysics low dimension microfluidic problem, the conventional Navier-Stokes (NS) approach is not a feasible solution due to failure in satisfying continuum hypothesis for mass and momentum conservation below 10 micron. Molecular dynamics (MD) simulations require more resources and more time while solving complex geometry. Incorporating and coupling multiphysics in a nano domain is also a serious challenge. A mesoscopic lattice Boltzmann method (LBM) is recently proved to be better methodology to model and investigate such devices due to its tremendous advantages like massive parallelism and easy incorporation of multiphysics. Complex fluid flows, including multi-phase flow, blood flow, particle suspension flow, binary mixtures, liquid crystals, and surface wetting flows have been successfully simulated using LBM [14], [15].The method solves Boltzmann equation from scratch and allows the particles to move on discrete lattices. The mass and momentum are locally conserved by streaming and collision among particles. The rest of the paper is organized as follows. In section 2, the simulation model is described with solved equations. The experiment details with fabrication flow and characterization is discussed in section 4. In section 5, the results are presented and analyzed followed by a conclusion in section 6.

II. LBM SIMULATION MODEL

A. LBM Hydrodynamics model

For the implementation of the two phase 3D lattice Boltzmann study, we used a standard D3Q19 (3 dimension 19 velocity vector) model as shown in Fig 1.The basic vectors of D3Q19 model are given by

$$\overline{e_i} = (\overline{e_1},\overline{e_2},\overline{e_3},\overline{e_4},\overline{e_5},\overline{e_6},\overline{e_7},\overline{e_{18}},\overline{e_9},\overline{e_{10}},\overline{e_{11}},\overline{e_{12}},\overline{e_{13}},\overline{e_{14}},\overline{e_{15}},\overline{e_{16}},\overline{e_{17}},\overline{e_{18}},\overline{e_{19}})$$

Now, the streaming and collision are two major process which leads to evolution of particle distribution function in the above nineteen predefined direction. This process is described by

$$f_i(\vec{x}+\vec{e}_i\delta_t, t+\delta_t) - f_i^t(\vec{x},t) = -\frac{f_i^t(\vec{x},t) - f_i^{eq}(\vec{x},t)}{\tau} \quad (1)$$

where i=0, 1,.. 18 and τ is the dimensionless relaxation time of Bhatnagar-Gross-Krook (BGK) collision operator[16]which is related to kinematic viscosity of the fluid.

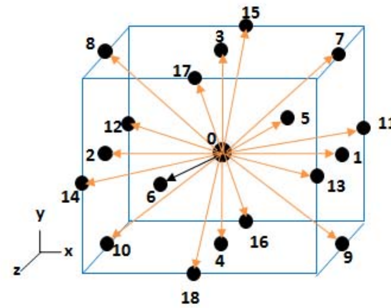

Fig. 1. Discrete velocity set of 3 dimensional 19-velocity (D3Q19) model.

Using the above distribution function, the macroscopic density and velocity are defined as

$$\rho(\vec{x},t) = \sum_{i=0}^{e_i} f_i^t(\vec{x},t) \quad (2)$$

$$\vec{u}(\vec{x},t) = \frac{1}{\rho}\sum_{i=0}^{e_i} f_i \vec{e_i} \quad (3)$$

For a linear elastic collision, a local equilibrium distribution function is defined as only the function of locally conserved mass and momentum density. It is given by

$$f_i^{eq}(\vec{x},t) = w_i\rho\left(1+\frac{3\bar{e}_i\bar{u}}{c^2}+\frac{9(\bar{e}_i\bar{u})^2}{2c^4}-\frac{3(\bar{u})^2}{2c^2}\right) \quad (4)$$

where c is the lattice space defined as the ratio of lattice spacing to lattice time step (Δx/ Δt). The lattice weights (w_i) are defined as

$$w_i = \begin{cases} 4/9 & i=0 \\ 1/9 & i=1,2,3,4 \\ 1/36 & i=5,6,7,8 \end{cases}$$

In LBM, the physical quantities must be converted into dimensionless lattice units. In our study, for simplicity, we consider Δx and Δt as unity which results in c=1. For the multiphase simulations, the SC-pseudo potential model [16]incorporates a non-local interaction among particles. The interaction force at each lattice site can be written as

$$F_\alpha = -G_{\alpha\alpha'}\psi^\alpha(x)\sum_i w_i\psi(x+c_i)c_i \quad (5)$$

where Ψ^α is the effective mass which is the function of local density and time and $G_{\alpha\alpha}$'(x,x') is the Green's function. The magnitude of the $G_{\alpha\alpha}$' determines the strength of interaction and its sign indicates whether the interaction is repulsive (cohesive force) or attractive (adhesive force). The macroscopic velocity is then updated with respect to force at the lattice point α as

$$\vec{u}(\vec{x},t) = u' + \frac{\tau}{\rho_\alpha} F_\alpha \quad (6)$$

where u' is the velocity obtained earlier. Now, the effective mass term $\Psi^\alpha(x)$ that exists in pseudopotential is proportional to the density term which is the function of time and position. So in order to bound the pseudo potential $\Psi^\alpha(x)$ for large density and to have it proportional to the smaller density, usually $\Psi^\alpha(x) = 1 - \exp(-\rho)$ is used. With this formulation, the multiphase simulation of density ratios up to 30 to 50 can be simulated. The interface between the domains of different fluid is assumed to have a finite width. So in order to capture the interface, the order parameter $\varphi = \rho_h - \rho_l$ is introduced. Finally, to implement partial wetting boundary on the walls, the densities on the walls (ρ_{wall}) must be specified because the interaction force accounts for the densities of neighbors alone. In order to tune the wetting, we propose the wetting parameter η_{wet} (0 to 1) to be introduced in the wall. So the following initial condition must be specified at a wall for desired wetting.

$$\rho_{wall} = \eta_{wet} * (\rho_h - \rho_l) + \rho_l \quad (7)$$

where ρ_h and ρ_l are densities of heavier fluid and lighter fluid respectively.

B. Algorithm of Computation

The algorithm of computation can be summarized as follows

Step 1: Initialize velocities (e_i), weights (w_i), relaxation time (τ) ,densities ρ_h, ρ_l, , and $G_{\alpha\alpha'}$.

Step 2: Define a periodic boundary condition, no-slip bounce back condition and partial wetting condition on the required walls. Thus geometry of the channel is defined here.

Step3: Compute particle distribution function for streaming and collision using equation (1).

Step4: Compute macroscopic density and macroscopic velocity using equation (2) and Equation (3) respectively.

Step5: Calculate $\Psi^\alpha(x)$ and interaction force using F_α equation (5).

Step6: Update the velocity using equation (6)

Step7: Advance one time step and return to Step3

C. Validation

In order to validate this modeling approach, we compare the numerical results with the benchmark known analytical results of Poiseuille flow of a fluid in a 3D channel of dimension(d) 30 x 30 x 30 (X x Y x Z) lattices is considered[17]. The flow is driven by the external force (F) acting on a fluid in X-direction. In this simulation, the top, bottom, front and back walls are defined as no slip solid walls with the partial wetting condition. The remaining left and right walls are defined as periodic. The velocity profile of the Poiseuille flow as shown in Fig.2 is given by the relationship as equation 8.

$$u(x) = \frac{F}{2\vartheta}(d^2 - y^2) \quad (8)$$

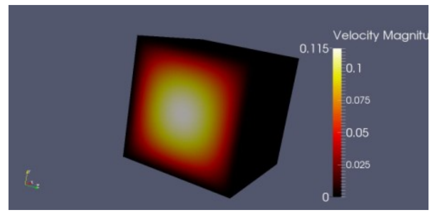

Fig. 2. 3D Screenshot of the simulated Poiseuille flow with body force applied on Y direction.

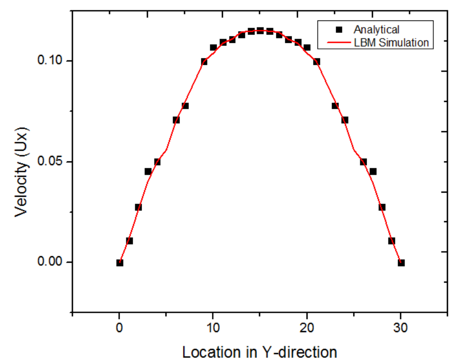

Fig. 3. Comparison of numerical results with the analytical solution for Poiseuille flow.

Fig.3 shows the agreement of numerical results with analytical solutions for the τ=0.8, F=2e-4. The agreement shows that LBM model can be used as a design tool for such analysis.

III. Experimental Details

A PDMS micromixing device is fabricated by the mold replica process. Generally, a UV-lithography based transferred pattern on SU-8 will be used as a mold for fabrication of such devices. But we skipped the expensive UV-lithography step by using a simple copper (Cu) layer printed on a printed circuit board (PCB) as a mold as shown in Fig.4. Thus, this method is relatively low cost approach than UV-lithography. Though this method has limitation in terms of the achievement of minimum feature size, it still can be explored to fabricate the microfluidic devices poses dimensions in atleast few tens or hundreds of microns. In this study, the minimum width of the fabricated microchannel is 250μm and depth is 70μm. The devices with these features are still can be exploited better for many low-cost Bio-MEMS applications.

A. Micromixer/Microchannel Fabrication

The micromixer patterns are carefully designed using Eagle PCB design software. The patterned PCB mold is fabricated commercially with Cu thickness of 70µm. An elastomer precursor (sylgard 184) and its curing agent are mixed in 10:1 ratio and degassed using desiccators. The solution is then poured over PCB-mold on flat surface in glass petridish and cured at 80°C for 40 min.

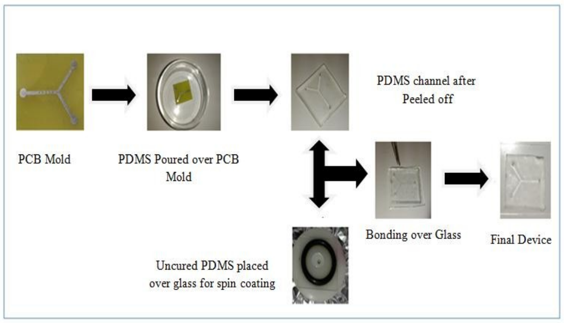

Fig. 4. Fabrication flow of low-cost micromixer.

After hardening, the replica is peeled off from mold, the reservoir holes were punched. The PDMS channels are then bonded to a glass slide using adhesive bonding technique. A fresh PDMS solution is uniformly spin coated on glass slide at 8000rpm for 8min. As a result an uncured PDMS thickness of 1 – 1.5µm is obtained on a glass substrate. Above fabricated PDMS micro channel is gently placed on the freshly coated glass surface without trapping air. Finally the device altogether then kept flat at 90°C for 15min to cure the adhesive bonding layer. Thus by using the above low cost technology we have also eliminated the requirement of expensive plasma bonding.

B. Characterization Setup

An in-house developed microfluidics characterization set-up is used for characterization of the fabricated device[18]. The complete setup consists of USB digital camera for capturing image/video in real time, XYZ stage for holding sample, Arm7 based electronic system which has standard circuits to provide actuation voltage for optional electro kinetic study (not used in this work) and to handle image processing along with HDMI display. The system is designed in real time embedded Linux platform and embedded with GUI. A simple C ++ and python scripts were written to trigger the camera and to capture and analyze the mixing. In order to calculate the mixing efficiency of the fabricated micromixers, the chains of images are captured using digital camera at 30frames/second. At first, the probability distribution function (PDF) is calculated by finding the probability values of the concentrated regions[19]. This is obtained by normalizing the each concentration pixel value (c_i^*) with the concentration of total evaluated region(c^*). Then the variance of the concentration is computed and normalized again with mean value to evaluate the mixing index using the equation 9.

$$MI = \sqrt{\frac{1}{N}\sum \frac{c_i^* - c^*}{c^*}} \qquad (9)$$

Finally the mixing efficiency is calculated as 1-MI. Thus, the mixing efficiency is calculated as homogeneity of mixed pixel density.

IV. Formulation of the Mixing Study

The methodology discussed in this work is summarized as a flow chart described below in Fig.5. At first, the geometry is designed using CAD tool. After optimization, the PCB layout is synthesized.

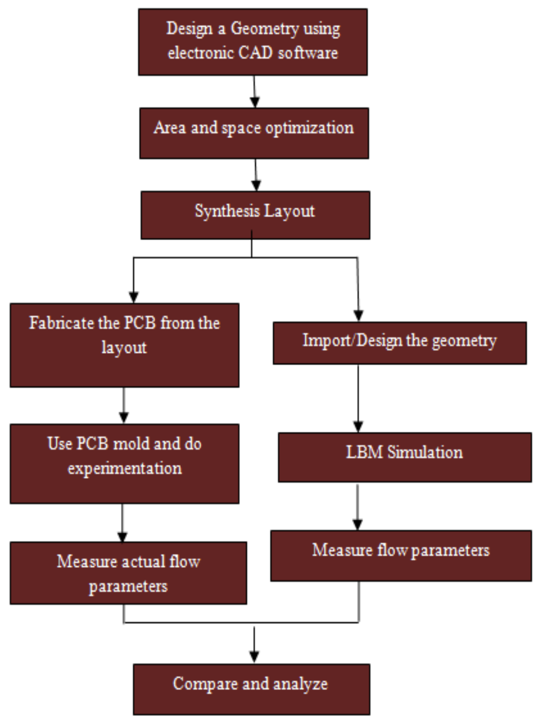

Fig. 5. Flow chart of the formulation of the problem.

The PCB layout is used as a mold to fabricate PDMS micromixers. The fabricated micromixers are explored for the mixing enhancement study. As usual for micromixers, two inlets and one outlet are designed. The six different passive micromixers with different obstacle pattern as shown in Fig.6 are fabricated and characterized using in-house developed characterization system. The obstacles are named as cross (pattern 1), triangle (pattern 2), Pentagon (pattern 3), star (pattern 4), Hexagon (pattern 5), I-shape (Pattern 6). The obstacle patterns are chosen due to the understanding that more the fluid exposed to edges better the chance of turbulence. At a same time, the geometry is imported into the LBM simulation and mixing efficiency is investigated.

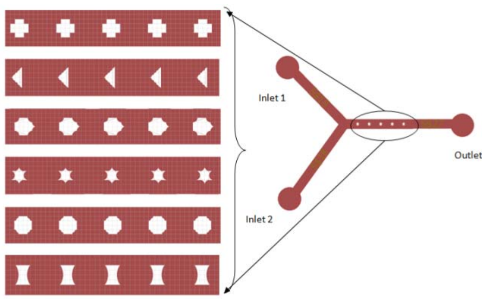

Fig. 6. Six obstacle patterns placed at the junction of Y mixers for mixing enhancement(one for each study)

V. RESULTS AND DISCUSSION

The targeted two different fluids are made to enter the mixing chamber through inlet1 and inlet2. The flow rates of both the fluids are fixed to be 0.1ml/hour using syringe pump. For simplicity the fluid1 and fluid2 are considered to be paper ink of blue and red color respectively as shown in Fig. 7.

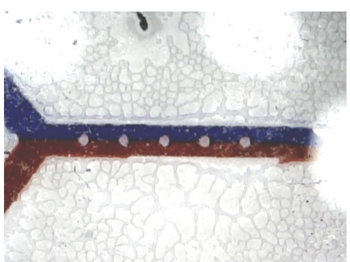

Fig. 7. Experimental mixing measurement

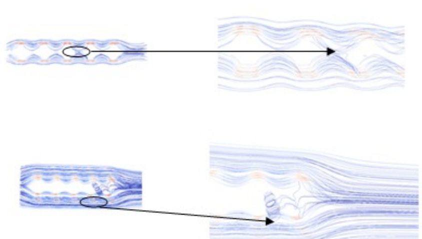

Fig. 8. Simulation result of vortices created due to a pattern pillar in micromixer.

As the fluid pass through the channel, due to the introduced obstacle the flow gets disturbed and resulted in turbulence inside the channel. Fig. 8 shows the vortices created due to the introduced patterned pillar obstacles at y junction. In each study, there are five obstacles placed to create chaotic turbulence. In all cases it is observed that the turbulence in flow happened only after atleast third obstacle. This shows that number of obstacles placed is crucial in these mixer designs. Then the mixing efficiency was calculated as per the above mentioned statistical approach at the output channel at steady state of the fluid. It was calculated on the plain channel point after five obstacles near outlet reservoir. The obtained results are tabulated in table 1. For simulation, the mixing efficiency is calculated by number of stream crossing across the width of the channel. From the obtained results, it can be observed that the pattern 1, and pattern 4 produced the maximum mixing efficiency. The reason for this is they posses more sharp edges which initiated the chaotic advection. It is also observed that pattern 6 also produced closer to maximum mixing efficiency though it does not possess many sharp edges. The reason for this may be that the area of the obstacle is larger. In order to design better mixer, the obstacle with sharp edges and larger area can be preferred however viscosity of the fluid also critical.

TABLE I. EXPERIMENTAL RESULTS OF MIXING EFFICIENCY

Obstacle Designed	Max.Mixing Efficiency obtained in %	
	Experiment	**Simulated**
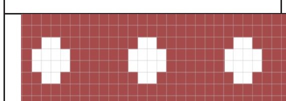	72.7	75
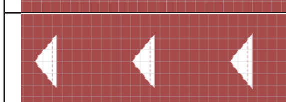	50.75	55
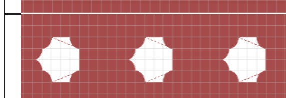	57.2	60
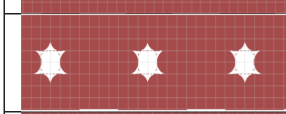	73.4	77
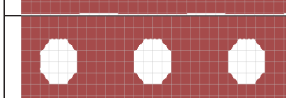	56.3	58
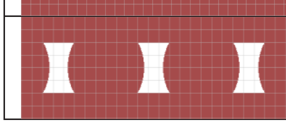	71.3	72

To explore this study further, a LBM-CAD tool is built and a simple graphical user interface (GUI) window is created using QT creator software as shown in Fig.9.

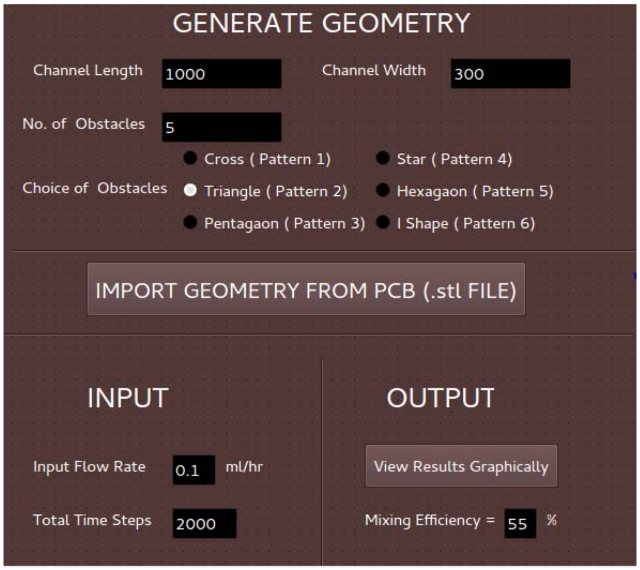

Fig. 9. GUI window of the LBM-CAD tool for mixing analysis

The GUI has options to generate or import the geometry. The input parameters are flow rate and total time steps and the output can be directly visualized graphically using visualization tool kit (vtk) files or simply get the computed mixing efficiency.

VI. Conclusion

In this work, a low cost approach to fabricate and characterize passive PDMS micromixers has been presented. The six different obstacle patterns in the channel are considered for mixing enhancement study. Each case is analyzed experimentally using an in-house developed low cost characterization setup. The mixing characteristics are also investigated using D3Q19 LBM model. The simulation results show agreement with the experimental results. Results show that the patterns posses more edges leads to maximum mixing efficiency. The time dependent mixing study can provide more insight. However, the presented results can be used to design better mixers for lab-on-chip applications.

References

[1] P. S. Dittrich and A. Manz, "Lab-on-a-chip: Microfluidics in drug discovery," *Nature Reviews Drug Discovery*, vol. 5, no. 3. pp. 210–218, 2006.

[2] S. Xing, R. S. Harake, and T. Pan, "Droplet-driven transports on superhydrophobic-patterned surface microfluidics," *Lab Chip*, vol. 11, no. 21, p. 3642, 2011.

[3] M. G. Pollack, R. B. Fair, and A. D. Shenderov, "Electrowetting-based actuation of liquid droplets for microfluidic applications," *Appl. Phys. Lett.*, vol. 77, no. 82, pp. 1725–1726, 2000.

[4] N. Shembekar, C. Chaipan, R. Utharala, and C. A. Merten, "Droplet-based microfluidics in drug discovery, transcriptomics and high-throughput molecular genetics," *Lab Chip*, vol. 16, no. 8, pp. 1314–1331, 2016.

[5] T. Pravinraj and R. Patrikar, "Splitting and transport of a droplet with no external actuation force for lab on chip devices, in: Commun. Comput. Inf. Sci., 2017: pp. 707–717. doi:10.1007/978-981-10-7470-7_66.

[6] T. Pravinraj and R. Patrikar, "Modeling and characterization of surface roughness effect on fluid flow in a polydimethylsiloxane microchannel using a fractal based lattice Boltzmann method," *AIP Adv.*, vol. 8, no. 6, 2018.

[7] W. Tseng, J. Lin, W. Sung, S. Chen, and G. Lee, "Active micro-mixers using surface acoustic waves on Y-cut 128 ◦ LiNbO 3," vol. 539, 2006.

[8] A. A. S. Bhagat, E. T. K. Peterson, and I. Papautsky, "A passive planar micromixer with obstructions for mixing at low Reynolds numbers," vol. 1017.

[9] V. Hessel, H. Löwe, and F. Schönfeld, "Micromixers — a review on passive and active mixing principles," vol. 60, pp. 2479–2501, 2005.

[10] M. Wang and Q. Kang, "Modeling electrokinetic flows in microchannels using coupled lattice Boltzmann methods," *J. Comput. Phys.*, vol. 229, no. 3, pp. 728–744, 2010.

[11] K. Horiuchi and P. Dutta, "Electrokinetic flow control in microfluidic chips using a field-effect transistor.," *Lab Chip*, vol. 6, no. 6, pp. 714–23, 2006.

[12] C. Lee, C. Lin, and L. Fu, "Passive Micromixers Theory of Lamination," no. 1, pp. 1–12, 2014.

[13] J. Friend and L. Yeo, "Fabrication of microfluidic devices using polydimethylsiloxane," pp. 1–5, 2010.

[14] H. Huang and X. Lu, "Relative permeabilities and coupling effects in steady-state gas-liquid flow in porous media: A lattice Boltzmann study," *Phys. Fluids*, vol. 21, no. 9, p. 092104, 2009.

[15] T. Pravinraj and R. Patrikar, "Modelling and investigation of partial wetting surfaces for drop dynamics using lattice Boltzmann method," *Appl. Surf. Sci.*, vol. 409, pp. 214–222, 2017.

[16] P. L. Bhatnagar, E. P. Gross, and M. Krook, "A model for collision processes in gases. I. Small amplitude processes in charged and neutral one-component systems," *Phys. Rev.*, vol. 94, no. 3, pp. 511–525, 1954.

[17] F. Mechanics, "Exercise 5 : Exact Solutions to the Navier-Stokes Equations I Example 1 : Plane Couette Flow Example 2 : Plane Poiseuille Flow (Channel Flow) Energy Dissipation in Poiseuille Flow," pp. 1–7, 2010.

[18] V. Jain, T. P. Raj, and R. Deshmukh, "Design, fabrication and characterization of low cost printed circuit board based EWOD device for digital microfluidics applications," *Microsyst. Technol.*

[19] G. Pendharkar and R. Deshmukh, "Investigation of surface roughness effects on fluid flow in passive micromixer," pp. 2261–2269,2014.